Acta Pharmaceutica Sinica B 2023;13(1):113−127

Chinese Pharmaceutical Association
Institute of Materia Medica, Chinese Academy of Medical Sciences

Acta Pharmaceutica Sinica B

www.elsevier.com/locate/apsb
www.sciencedirect.com

ORIGINAL ARTICLE

Dihydrotanshinone I preconditions myocardium against ischemic injury *via* PKM2 glutathionylation sensitive to ROS

Xunxun Wu[a], Lian Liu[a], Qiuling Zheng[b], Hui Ye[a,c], Hua Yang[a,*], Haiping Hao[a,b,*], Ping Li[a,*]

[a]*State Key Laboratory of Natural Medicines, Department of Pharmacognosy, School of Traditional Chinese Pharmacy, China Pharmaceutical University, Nanjing 210009, China*
[b]*College of Pharmacy, China Pharmaceutical University, Nanjing 210009, China*
[c]*State Key Laboratory of Natural Medicines, Jiangsu Provincial Key Laboratory of Drug Metabolism and Pharmacokinetics, China Pharmaceutical University, Nanjing 210009, China*

Received 5 February 2022; received in revised form 4 April 2022; accepted 12 May 2022

KEY WORDS

Dihydrotanshinone I;
Ischemic preconditioning;
PKM2;
Glutathionylation;
Myocardial ischemia;
ROS;
Oxidation modification;
Nuclear translocation

Abstract Ischemic preconditioning (IPC) is a potential intervention known to protect the heart against ischemia/reperfusion injury, but its role in the no-reflow phenomenon that follows reperfusion is unclear. Dihydrotanshinone I (DT) is a natural compound and this study illustrates its role in cardiac ischemic injury from the aspect of IPC. Pretreatment with DT induced modest ROS production and protected cardiomyocytes against oxygen and glucose deprivation (OGD), but the protection was prevented by a ROS scavenger. In addition, DT administration protected the heart against isoprenaline challenge. Mechanistically, PKM2 reacted to transient ROS *via* oxidization at Cys423/Cys424, leading to glutathionylation and nuclear translocation in dimer form. In the nucleus, PKM2 served as a co-factor to promote HIF-1α-dependent gene induction, contributing to adaptive responses. In mice subjected to permanent coronary ligation, cardiac-specific knockdown of *Pkm2* blocked DT-mediated preconditioning protection, which was rescued by overexpression of wild-type *Pkm2*, rather than Cys423/424-mutated *Pkm2*. In conclusion, PKM2 is sensitive to oxidation, and subsequent glutathionylation promotes its nuclear translocation. Although IPC has been viewed as a protective means against reperfusion injury, our study reveals its potential role in protection of the heart from no-reflow ischemia.

*Corresponding author.
E-mail addresses: liping2004@126.com (Ping Li), hhp_770505@hotmail.com (Haiping Hao), yanghuacpu@126.com (Hua Yang).
Peer review under responsibility of Chinese Pharmaceutical Association and Institute of Materia Medica, Chinese Academy of Medical Sciences.

https://doi.org/10.1016/j.apsb.2022.07.006

1. Introduction

Myocardial ischemia is still a life-threatening disease due to the lack of effective therapeutics. Once acute coronary occlusion occurs, the immediate remedy is to remove the occlusion through thrombolytic or mechanical means. However, the restoration of blood supply can induce further heart damage beyond that of the initial ischemic injury known as ischemia/reperfusion injury[1]. As a result, ischemic preconditioning (IPC) emerges as one of the potential interventions known to protect the heart against ischemic and reperfusion injury[2]. As a means of preconditioning, several minutes of acute coronary occlusion followed by reperfusion delay the onset of myocardial infarct from a subsequent period of prolonged lethal ischemia[3]. Through activation of complex signaling cascades, IPC is proven to reduce infarct size and post-ischemic contractile dysfunction[4]. Although percutaneous coronary intervention is a pivotal step in the current management of myocardial infarction, this intervention still faces the situation that after relieving the proximal epicardial coronary occlusion, blood flow to the cardiac tissues may still be impeded, a phenomenon known as no-reflow that is associated with increased cardiac complications and a poor prognosis[5,6]. Indeed, experimental studies and clinical data have clearly shown that no-reflow occurs after reperfusion with a variable prevalence[7]. The protective effects of IPC on reperfusion injury have been well documented; however, whether preconditioning protects the heart with no-reflow is unclear. More studies demonstrate that no-reflow, at least in some patients, is reversible[8], thus creating a new possibility for the search of no-reflow from the aspect of preconditioning protection.

When oxygen is deprived, energy metabolism is shifted away from mitochondrial oxidation to glycolysis, an adaptive response to limit oxygen consumption. Pyruvate kinase (PK) is an enzyme that catalyzes the conversion of phosphoenolpyruvate to pyruvate in glycolysis, and is considered as a critical determinant of glycolytic reprogramming[9]. In cancer cells, to meet the increased biosynthetic demands, pyruvate kinase isoform M2 (PKM2) diverts glucose into anabolic pathways[10]. Moreover, metabolic and nonmetabolic roles of PKM2 are also elucidated in non-cancerous cells. In mice subjected to stroke, recombinant PKM2 administration reduced infarct volume and improved neurogenesis[11]. In addition, PKM2 is shown to regulate cardiomyocyte recycle and regeneration[12]. PKM2 shuttles between the cytosol and nucleus, which is sensitive to redox regulation and chemical modification[13]. Different from the enzymatic role in the cytosol, PKM2 in the nucleus functions as a co-activator for transcriptional regulation of genes associated with cell growth, metastasis and apoptosis[14]. Hypoxia-inducible factor 1α (HIF-1α) is a transcription factor that can be activated under hypoxic conditions for gene induction involved in metabolism and cell survival[15,16]. PKM2 in the nuclear promotes transactivation of HIF-1α target genes[17], which indicates the potential in the regulation of adaptive responses.

Excessive reactive oxygen species (ROS) generation is no doubt injurious; however, transient ROS generation can activate cell survival programs and increase the tolerance to ischemic injury[18]. Exposure to low level ROS can produce beneficial effects in IPC[19,20], and enhanced antioxidant defense is a mechanism for preconditioning protection. ROS is both necessary and sufficient to stabilize and activate HIF-1α. The effects of ROS on HIF-1α protein stability are a lively scientific debate. Earlier evidence on ROS regulation primarily focused on HIF-1α stabilization *via* direct prolyl hydroxylase domain-containing (PHD) inhibition under normoxia[21]. In addition, it has been suggested that ROS deprives the PHD activity probably by oxidizing its necessary cofactor: ferrous iron[22,23]. However, despite extensive investigation, the precise mechanisms by which ROS mediates HIF-1α stabilization remain incomplete. To this end, glutathionylation is a reversible post-translational modification that occurs to cysteine residues when exposed to ROS. In fact, *S*-glutathionylation modification is a way to prevent protein from further oxidative degradation[24]. Oxidative modification of Cys358 degrades PKM2 from tetrameric form to a dimeric form[10]. PKM2 dimer is capable of entering the nucleus, raising the possibility that *S*-glutathionylation promotes PKM2 entry in the nucleus for transcriptional regulation under stress.

Dihydrotanshinone I (DT) and analogs are bioactive components derived from the dried root and rhizome of *Salvia miltiorrhiza,* which is a medicinal herb that has been used in the treatment of cardiovascular diseases. Since 2000, 39 clinical trials have been performed to test the clinical benefits of *S. miltiorrhiza* in the treatment of cardiovascular diseases. DT, as one of the key components in *S. miltiorrhiza*, has been suggested as a promising chemical template for the development of preconditioning drugs[25]. However, the exact mechanisms by which DT elicits cardioprotection and particularly the preconditioning effects remain unclear[26,27]. Previously, we demonstrated that DT generates transient ROS from mitochondria and stabilizes HIF-1α to enhance anti-oxidative defense, contributing to the attenuation of ischemia−reperfusion injury through preconditioning protection[28,29]. In view of the detrimental role of no-reflow in cardiovascular diseases, this study investigated whether DT protected the heart against ischemic insult *via* a preconditioning mechanism. Herein, PKM2 is shown as a sensor to ROS signaling in cardiomyocytes. DT induced modest ROS production and promoted PKM2 glutathionylation. This modification is essential for PKM2 nuclear translocation wherein it interacts with HIF-1α to rescue cell survival. Although preconditioning has been viewed as a protective means against reperfusion injury, our study reveals its potential role in the protection of heart ischemia in the no-reflow setting.

2. Materials and methods

2.1. Reagents

Dihydrotanshinone I (purity $\geq$ 98%) was obtained from Chengdu MUST Biological Technology Co., Ltd. (Chengdu, China). Anti-PKM2 antibody (cat#4053), anti-Lamin A/C antibody (cat# 2032) and anti-HIF-1α antibody (cat#36169) were purchased from Cell Signaling Technology (Danvers, MA, USA). Anti-DDDDK tag antibody (cat#20543-1-AP), anti-PCNA antibody (cat#10205-2-AP), anti-importin A5 (cat#18137-1-AP), anti-PKM2 antibody

(cat#60268-1-Ig), anti-cardiac troponin T antibody (cat#15513-1-AP), anti-GAPDH antibody (cat#60004-1-Ig), goat anti-rabbit IgG (cat#SA00001-2), anti-GLRX antibody (cat#15804-1-AP) and goat anti-mouse IgG (cat#SA00001-1) were obtained from Proteintech (Wuhan, China). Alexa Fluor 594 (cat#ab150116), alexa-fluor 488 (cat#ab150077), anti-glutathione antibody (cat#ab19534), mito-TEMPOL (cat#ab144644) and cycloheximide (cat#ab120093) were obtained from Abcam (Cambridge, UK). Anti-FLAG magnetic beads (cat#M8823), wheat germ agglutinin (cat#L9640), diamide (cat#D3648), isoprenaline (cat#I5627) and *N*-acetylcysteine (cat#A7250) were obtained from Sigma−Aldrich (St. Louis, MO, USA).

2.2. Ethics statement

Animal experiments were carried out under the authorization of Chinese Experimental Animal Administration and legislation of China Pharmaceutical University (Approval No. 2020-01-008). All animals were allowed free access to food and water for 1 week before experiments. At the end of the experiment, animals were euthanized by cervical dislocation.

2.3. Animals and treatment

Male C57BL/6 mice (4-week-old) were obtained from the Comparative Medical Center of Yangzhou University (Yangzhou, China). Male Sprague−Dawley rats (7−8-week old, 200−220 g) were obtained from Shanghai Sippr-BK Laboratory Animal Co., Ltd. (Shanghai, China).

In the isoprenaline (ISO)-induced myocardial damage model, rats were administered DT (5 mg/kg), acetylcysteine (NAC, 200 mg/kg) or both by gavage for 3 consecutive days as preconditioning treatment. Then, rats were subjected to subcutaneous injection (65 mg/kg) for 2 consecutive days, and the examination was performed 24 h after the last injection.

For *Pkm2* knockdown (KD) or overexpression (OE) in mouse heart, the adeno-associated virus (AAV9) delivery system was used to deliver AAV9-cTnT-sh*Pkm2*, AAV9-cTnT-wildtype *Pkm2*, AAV9-cTnT-mutants *Pkm2*. In brief, 5-week-old male C57BL/6 mice were administered 200 μL of virus containing 4×10^{11} AAV9 vector genomes containing *Pkm2* shRNA, scrambled shRNA, wildtype *Pkm2* or *Pkm2* mutants (Vigene Biosciences Co., Ltd., Shandong, China) *via* the tail vein. Western blotting analysis was adopted to confirm the knockdown and overexpression efficiencies. Before coronary ligation, heart tissue was collected to examine preconditioning regulation in the heart after a three-day pre-treatment with DT (10 mg/kg/day).

For the preparation of permanent coronary ligation, mice were pre-treated with DT (10 mg/kg/day) for 3 consecutive days before coronary ligation and then anesthetized with sodium pentobarbital (50 mg/kg, i.p.). Following tracheal intubation and thoracotomy, ischemia was initiated by a complete ligation of the left anterior descending coronary artery with a 7-0 silk ligature. Heart tissue was examined for myocardial infarction after coronary ligation without reperfusion three days after ligation. At three weeks after surgery echocardiography was performed with a Vevo 3100LT micro-ultrasound system (Visual Sonics Inc, Toronto, Ontario, Canada). The left ventricular function parameters including ejection fraction (EF) and fractional shortening (FS) were recorded according to the M-mode images acquired.

The levels of lactate dehydrogenase (LDH), cardiac troponin (cTn-I) and creatine kinase isoenzyme-MB (CK-MB) in the blood were determined using commercial kits (DOJINDO Laboratories, Shanghai, China; cusabio, Wuhan, China).

2.4. Cell culture, cell transfection and stable cell line construction

HL-1 cells (Jennio Biotech Co., Ltd., Guangzhou, China), H9C2 and HEK293T cells (Cell Bank of the Chinese Academy of Sciences, Shanghai, China) were cultured in DMEM (KeyGEN Biotech, Nanjing, China) supplemented with 10% fetal bovine serum (FBS, Gibco, South America) in humidified 5% CO_2 at 37 °C.

For the overexpression experiments, wild-type or mutant *Pkm2* plasmids were transfected into 293T cells with Lipofectamine 3000 transfection reagent (Invitrogen, L3000008, USA).

Lentivirus were produced in HEK-293T cells by co-transfection with a three-plasmid lentivirus packaging system. DNA for transfection were prepared by mixing 600 ng psPAX2, 200 ng pMD2.G and 800 ng pLKO.1 with shRNA (or lenti-CRISPR v2 with sgRNA) plasmids. Viral supernatants were harvested at 48 and 72 h post-transfection. The viral supernatants were applied to HL-1 cells for 24 h supplemented with 8 μg/mL polybrene before replacement with normal growth media plus puromycin (2 μg/mL) for 7 days. The sgRNA and shRNA sequences are listed in Supporting Information Table S1.

2.5. Immunofluorescence staining

H9C2 cells were seeded in a cell imaging dish and fixed with 4% paraformaldehyde solution, followed by blocking with 5% FBS (dilute with 0.3% Triton X-100 in PBS). Cells were then incubated with primary antibodies (anti-PKM2, 1:300, Proteintech, cat#60268-1-Ig; anti-HIF-1α, 1:200, CST, cat#36169) overnight, followed by incubation with Alexa Fluor-conjugated secondary antibodies (Alexa Fluor 594, 1:500, Abcam, cat#ab150116; Alexa Fluor 488, 1:500, Abcam, cat# ab150077) for 1 h at room temperature. Cells were incubated with DAPI (Abcam, cat#ab104139) for 5 min at room temperature after washing for three times (total 15 min). The cells were imaged *via* a DeltaVision Ultra microscopic (GE Life Science, Boston, MA, USA).

2.6. Cross-linking of PKM2

The cross-linking analysis was conducted with intact cells. Briefly, in HL-1 cell culture, 2.5-mmol/L disuccinimidyl suberate (DSS, cat#21655, ThermoFisher Scientific, Waltham, MA, USA) was used to cross link for 30 min with constant rotation at 37 °C. Loading buffer then was added and the samples boiled for 10 min.

2.7. Analysis of intracellular ROS production and cell survival

Treated HL-1 cells were washed three times and incubated with DMEM medium containing 10 μmol/L H2DCFDA (cat#HY-D0940) at 37 °C for 30 min. The cells then were washed three times with warm DMEM medium and intracellular ROS production was detected by flow cytometry (CytoFLEX, Beckman Coulter Co., Ltd., USA). The cell survival rate was measured by a cell counting kit (CCK) 8 kit (cat#CK04, Dojindo, Japan).

2.8. Immunoprecipitation

Treated cells in 100 mm dishes were washed and lysed with 700 μL NP-40 lysate buffer. Lysates were centrifuged (12,000 ×

g, 10 min, 4 °C) and the protein concentration was determined. IgG or relevant primary antibody (4 μL) was added to 200 μg protein and incubated with mixing at 4 °C overnight. Lysates were transferred to tubes with 40 μL protein A/G magnetic agarose (cat#78609, ThermoFischer Scientific, Waltham, MA, USA) and incubated with mixing at 4 °C for another 3 h. The magnetic agarose was washed 4 times with NP-40 lysate buffer and 100 μL loading buffer was added and the samples boiled for 10 min for immunoblotting analysis.

2.9. Detection of cysteine sulfenic acid of PKM2

PKM2 cysteine sulfenic acid was detected by DCP-Bio1 probe (cat#NS1226, Merck, Darmstadt Germany). Briefly, treated HL-1 cells were lysed in DCP-Bio1 lysis buffer. Lysates were centrifuged at 12,000 × *g* for 10 min (4 °C), after which the supernatants were incubated with 1 mmol/L DCP-Bio1 probe for 2 h. Ultrafiltration was performed to remove the DCP-Bio1 probe, after which 100 μL of loading buffer was added and boiled for 10 min for immunoblotting analysis. Streptavidin−agarose beads (cat#88817, ThermoFisher Scientific, Waltham, MA, USA) were incubated overnight at 4 °C. The beads were then washed using NP-40 buffer and boiled for 10 min in loading buffer followed by Western blotting.

2.10. SA-GSSG pull-down assay

Recombinant PKM2 was incubated with SA-GSSG (0.5−1 mmol/L) for 2 h at 4 °C, and the reactions were terminated by adding loading buffer followed by boiling for 10 min.

2.11. Dual-luciferase reporter assay and quantitative real-time PCR

Cells were transfected with *Hif1a* and *Renilla* luciferase reporter plasmids for 24 h and then assayed according to the protocol. *Firefly* and *Renilla* luciferase activities were determined using dual luciferase assay kit (cat#DL101-01, Vazyme Biotech, China) in a Berthold TriStar[2] SLB 929 modular monochromator multimode reader (Berthold Technologies, Germany).

For total RNA extraction, reverse transcription and Q-PCR experiments, commercial kits (cat#R401-1, R223-1, Q121-1, Vazyme Biotech) were adopted and performed using the LightCycler480 q-PCR system (Roche, Basel, Switzerland). Internal reference (18S) and related primer sequences are listed in Supporting Information Table S2.

2.12. Molecular docking

The protein structure for docking analysis was downloaded from the protein data bank (PDB ID 1t5a). The leDock software (http://lephar.com) was employed to generate the docked conformation for GSSG bound to PKM2. The binding site of GSSG was defined as proteinaceous residues located within a distance of 4 Å radius from GSSG.

2.13. Histological analysis

For histopathological and fibrosis evaluation, 5-μm thick heart sections were stained with H&E and Masson's trichrome. Cardiac Troponin T (Proteintech, cat#15513-1-AP) and wheat germ agglutinin (WGA, cat#W6748, Thermo Fischer Scientific, Waltham, MA, USA) were detected by immunohistochemistry (IHC) staining. Fluorescent images were captured with a Zeiss 800 confocal microscope (Zeiss, Germany). For the examination of heart ischemic injury, the tissue was collected from the infarction border zone.

2.14. Statistical analysis

The between-group variances were similar and the data were normally distributed. Comparisons between groups were performed using one-way ANOVA (Tukey's multiple comparisons test) with GraphPad Prism 6.01 (Graphpad Software, Inc., San Diego, CA, USA). All data are expressed as means ± standard error of mean (SEM), except the proteome study, which used an unpaired two-tailed Student's *t*-test. Statistical significance was set at $^{*}P < 0.05$, $^{**}P < 0.01$, $^{***}P < 0.001$ and n.s., statistically not significant.

3. Results

3.1. DT preconditioning protects the heart from insult injury

Our previous study showed that DT protects cardiomyocytes through eliciting mild ROS production[28]. The HL-1 cell line derived from mouse cardiac tissue retains phenotypic characteristic of adult cardiomyocytes; the potency of DT on ROS generation was examined in this HL-1 cell line. H_2O_2 was shown to maintain cell survival at low concentrations (10 and 20 μmol/L), but exerted an injurious effect at high concentrations (Supporting Information Fig. S1A). By examining the concentrations and time courses, we confirmed that pre-treatment with 1−2 μmol/L DT for 4−8 h maintained cell survival with oxygen and glucose deprivation (OGD) insult (Fig. S1B). DT treatment (1 and 2 μmol/L) for 4 h induced modest ROS production, which was comparable to H_2O_2 treatment at low concentrations (10 and 20 μmol/L) (Fig. 1A). To verify this protection, the impact of H_2O_2 on cell survival was examined, and it was confirmed that H_2O_2 pre-treatment at low concentrations could protect cells from OGD. Thus, to observe the preconditioning effects, cells were pretreated with DT for 4 h. After washing, cells were exposed to OGD, and DT pre-treatment effectively maintained cell survival, but the effect was diminished by co-treatment with the ROS scavenger *N*-acetyl-L-cysteine (NAC) (Fig. 1B). These results suggest that ROS production maintained at a lower level was capable of protecting cells, presumably *via* preconditioning. Further study was undertaken to investigate the protective effect of DT in rats challenged by isoprenaline (ISO) (Fig. S1C), which induces heart injury owing to thrombosis associated with oxidative stress and an inflammation-related mechanism[30]. DT (5 mg/kg) was orally administered for 3 days before ISO challenges as a preconditioning treatment. DT administration reduced the ratio of heart weight to body weight (HW/BW) in ISO-treated mice, probably due to reducing edema in the heart, but not in the group treated with NAC (Fig. 1C). HE staining indicated that DT pretreatment reduced the infarct region, but the effects were compromised by co-treatment with NAC (Fig. 1D and E). Cardiac troponin T (c-TnT) is a marker of cardiomyocytes[31], and WGA staining is used to show the cell morphology[32]. Immunofluorescence staining of c-TnT and WGA showed ISO-induced pathological ventricular hypertrophy, which was indicated by increased cross-sectional area of cardiomyocytes. However, the anti-hypertrophic effect of DT was nullified by NAC treatment (Fig. 1F and G). Despite the observation

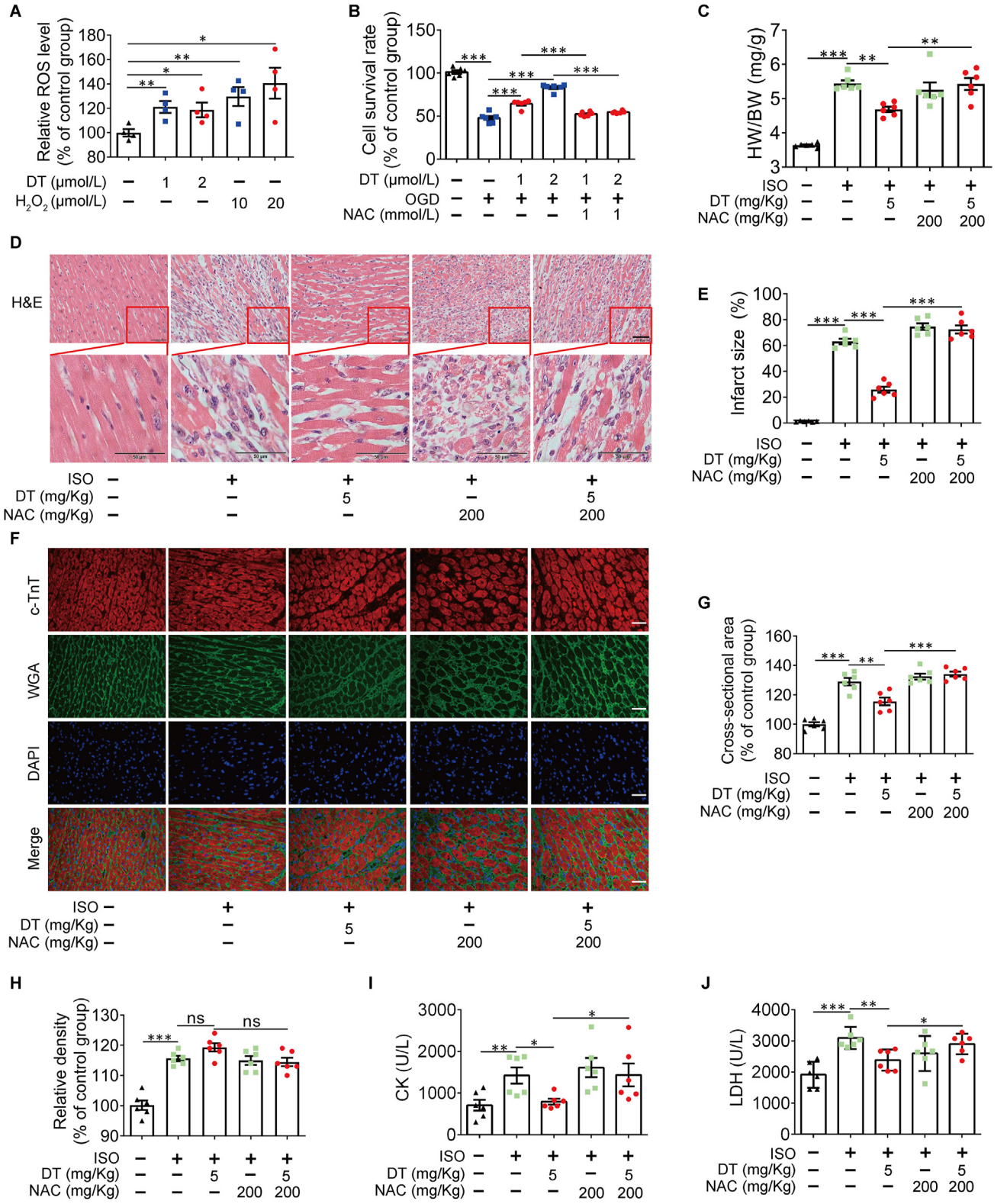

Figure 1 DT preconditioning protects the heart from damaging insult. (A) ROS production in HL-1 cells treated with DT or H_2O_2 for 4 h ($n = 4$). (B) Cell viability was measured by a CCK-8 assay ($n = 6$). (C) The ratio of heart weight to body weight (HW/BW) ($n = 6$). (D) H&E staining in heart sections ($n = 6$). Scale bar: 50 μm. (E) Calculated infarct size of the myocardium ($n = 6$). (F) Immunofluorescence staining of wheat germ agglutinin (WGA) and cardiac troponin T (c-TnT), ($n = 6$). Scale bar: 50 μm. (G) Cross-sectional area of cardiomyocyte ($n = 6$). (H) Quantitative analysis the content of c-TnT ($n = 6$). (I) creatine kinase (CK) in the blood. (J) Lactate dehydrogenase (LDH) in the blood ($n = 6$). The results are expressed as the mean ± SEM; $^*P < 0.05$, $^{**}P < 0.01$, $^{***}P < 0.001$. ns, statistically not significant.

that c-TnT content in the ISO group was slightly increased, no significant difference was detected between treatment groups (Fig. 1H). DT pre-treatment reduced elevated levels of circulating CK and LDH. However, co-treatment with NAC attenuated the action (Fig. 1I and J). All these results indicate the preconditioning role of DT in cardioprotection.

3.2. *DT promotes PKM2 nuclear translocation*

Our previous study indicated that DT treatment stimulated mild ROS release and stabilized HIF-1α, but the precise target and mechanism are unclear[28]. IPC has two distinct windows of cardioprotection: the first window occurs immediately after the IPC stimulation and the second window follows in 12−24 h with the regulation of nuclear transcription factors[33]. Since HIF-1α is mainly localized in the nucleus for transcriptional regulation, we performed a proteomic study with nuclei isolated from cardiomyocytes pretreated with DT for 12 h to find the potential mediators and transcriptional regulation. A total of 20,998 unique peptides and 4902 proteins were identified by proteomic analysis. The proteins were quantified with I Quant software and significant differences were defined with $P < 0.05$. In total, 1896 proteins were differentially distributed in the DT-*vs*-control comparison (Supporting Information Table S3). Those proteins with significant differences were assigned to KOG categories to determine their functional classifications and they were mainly associated with signal transduction and transcription (Fig. S1D). Differential protein pathway functional enrichment showed that genes for cardiovascular diseases, translation and signal transduction were highly enriched (Fig. S1E). Importantly, KEGG enrichment analysis showed the involvement of the HIF-1 signaling pathway in the biological action of DT (Fig. 2A), consistent with our previous finding that DT increased nuclear localization of HIF-1α[28]. Proteins with significant differences in enrichment are presented in a volcanic map, and the top 12 candidates are listed (Fig. 2B, and Fig. S1F). Of these, pyruvate kinase was top-ranked. Further analysis of unique peptides revealed isoform 2 of pyruvate kinase PKM (Fig. S1G and S1H), which indicates the potential role of PKM2 in DT action.

As DT-induced inhibition of mitochondrial complex I was shown to induce preconditioning regulation[28], the impact of PKM2 was examined; we found that PKM2 knockout increased complex I activity in HL-1 cells (Supporting Information Fig. S2A). This result indicates metabolic flexibility between glycolysis and mitochondrial oxidation. To verify that DT could directly interact with PKM2, surface plasmon resonance (SPR) experiments were conducted and showed that the K_D between DT and PKM2 was 56.8 μmol/L (Fig. S2B), which was much higher than the effective concentration (1 μmol/L) in previous *in vitro* experiments[28]. This result suggests that DT interacts with PKM2 in an indirect way. In addition, treatment with DT for 4 h had no impact on the expression of *Pkm2*, despite the induction observed at 24 h (Fig. 2C and Fig. S2C). Similar regulation was also observed in protein expression (Fig. 2D and Fig. S2D). Because PKM2 is a nucleoplasmic shuttling protein, its subcellular localization was investigated *via* treatment with DT. Immunoblotting revealed that treatment with DT for 4 and 24 h could induce the nuclear translocation of PKM2 (Fig. 2E and Fig. S2E). PKM2 dimer, but not tetramer, is favored to be translocated to the nucleus[34]. A DSS cross-linking assay supported the nucleus translocation of PKM2 after DT treatment. Western blot results indicate that DT treatment reduced PKM2 tetramer abundance and increased the dimer form (Fig. 2F). PKM2 tetramer, rather than the dimer, resides in the cytoplasm and is responsible for its enzymatic activity. DT promoted PKM2 nuclear translocation in dimer form, explaining its inhibitory effect on PK activity (Fig. 2G). To verify whether the preconditioning effect of DT depended on the PKM2 signaling pathway, a *Pkm2* knockout stable cell line was established (Fig. S2F). Cardiomyocytes were pretreated with DT for 4 h and after washing, cells were exposed to OGD. DT pretreatment maintained cell survival in a manner dependent on PKM2 (Fig. 2H). Collectively, these results raise the possibility that DT facilitates PKM2 nuclear import to trigger preconditioning effect.

3.3. *DT stabilizes HIF-1α and is dependent on nuclear PKM2*

PKM2 in the nucleus serves as a cofactor to facilitate HIF-1α transactivation[17]. An immunoprecipitation (IP) assay showed that DT treatment potentiated the interaction between HIF-1α and PKM2 (Fig. 3A). Consistently, DT treatment increased HIF-1α accumulation, but the action was abrogated in *Pkm2* knockout cells (Fig. 3B). In addition, an IP assay further confirmed the binding of PKM2 to HIF-1α inside the nucleus (Fig. 3C). As HIF-1α protein abundance is mainly controlled by protein stability, we speculate that HIF-1α accumulation by DT may be caused by a change in protein stability. When protein synthesis was inhibited by cycloheximide (CHX), DT decreased the degradation rate of both endogenous and over-expressed HIF-1α (Fig. S2G and Fig. 3E), while the mRNA level of *Hif1a* was not increased (Fig. 3F). In support, DT inhibited ubiquitination-dependent degradation of HIF-1α (Fig. 3D). A luciferase reporter assay confirmed that DT increased the activity of the *Hif1a* promoter, but the effect was blocked by *Pkm2* silencing (Fig. 3G). *Il10*, *Hmox1*, *Pdk1* and *Vegfa* are HIF-1α-targeted genes involved in preconditioning regulation[17,34−36] and DT increased their induction in a manner dependent on PKM2 (Fig. 3H).

Importin α5 (encoded by *Kpna1* gene) mediates the nuclear translocation of PKM2[37], while the shuttle of HIF-1α between cytoplasm and nucleus is mediated by importins 4 and 7[38]. Pretreatment with DT protected the cells from OGD insult, but the effect was lost in *Kpna1* knockout cells (Supporting Information Fig. S3A and S3B). Consistently, *Kpna1* knockout was predicted to reduce the nuclear translocation of PKM2 and nuclear HIF-1α accumulation (Fig. S3C). These results indicate that the nuclear translocation of PKM2 is required for DT to improve HIF-1α stability. It is proposed that *Pkm2* is a direct HIF-1α target gene and the alternative isoenzymes are controlled by HIF-1α[39]. However, in our case, *Hif1a* knock down (Supporting Information Fig. S4A) had a negligible effect on nuclear accumulation of PKM2 (Fig. S4C and S4D). In contrast, *Hif1a* knock down largely abolished the preconditioning effect of DT (Fig. S4B). These results suggest that PKM2 acts at the upstream of HIF-1α in the signaling cascades.

3.4. *The interaction of PKM2/HIF-1α is sensitive to ROS*

Our previous study showed that DT could induce transient mitochondrial ROS production[28]. We asked whether ROS mediated DT's action to promote PKM2 nuclear translocation *via* oxidative modification. Co-treatment with ROS scavenger mito-tempol (Mito-T), tiron or dithiothreitol (DTT), could largely abolish the effect of DT on stabilization of HIF-1α and induction of PKM2 nuclear translocation (Fig. 4A, Supporting Information Fig. S5A and S5B), and these effects were further confirmed by

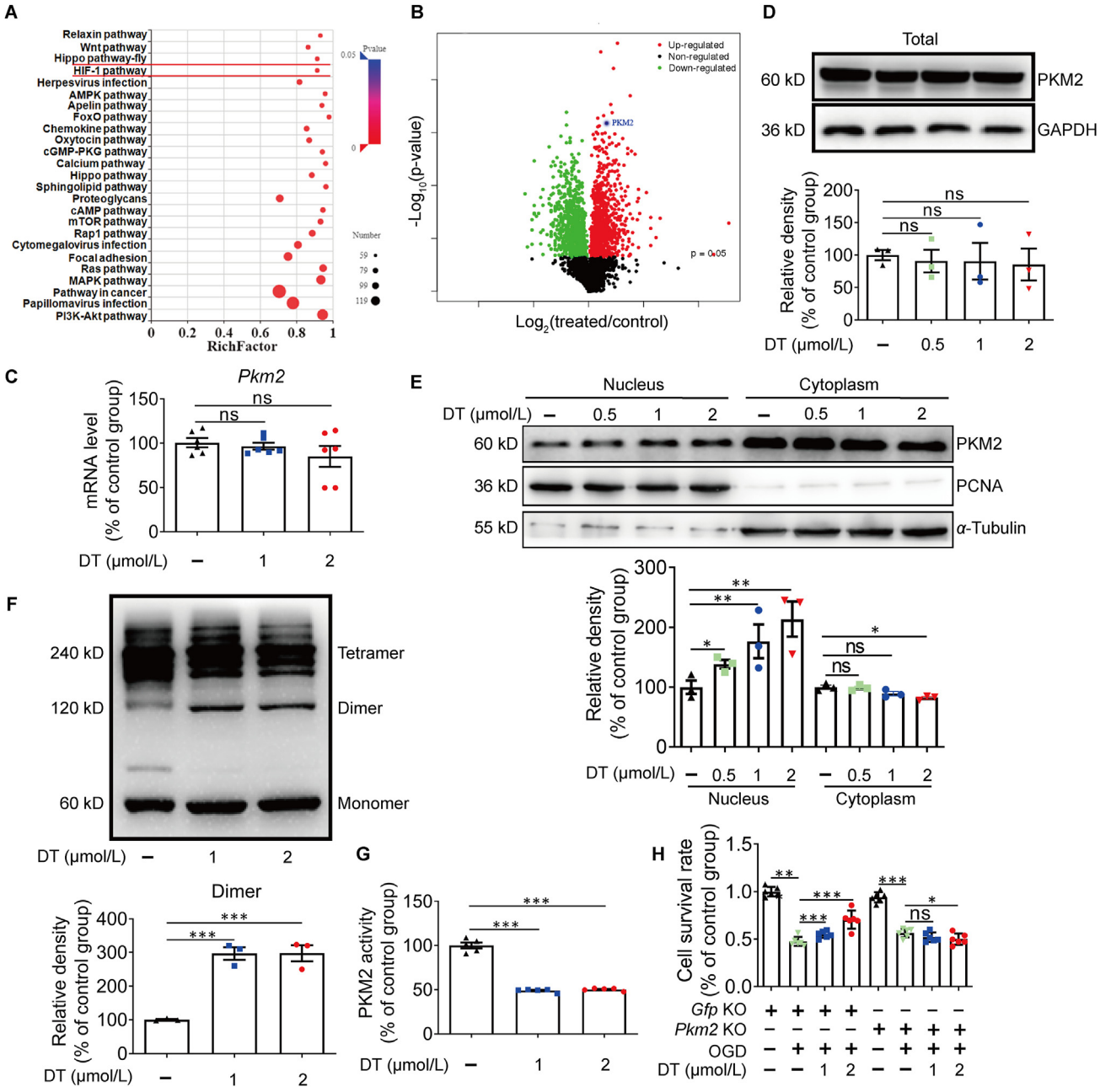

Figure 2 DT induces the nuclear translocation of PKM2. (A) KEGG enrichment of results from an iTRAQ study. Proteins with a P value < 0.05 (unpaired two-tailed Student's t-test) were assigned as differential protein. KEGG enrichment was performed and the twenty-five most significantly regulated pathways are listed; (B) A volcano plot shows the mean difference of the protein plotted against the P value (unpaired two-tailed Student's t-test, $P < 0.05$). (C) mRNA level of *Pkm2* was determined by quantitative PCR after treatment with DT for 4 h ($n = 6$). (D) Immunoblot analysis of PKM2 in HL-1 total cell extracts after treatment with DT for 4 h ($n = 3$). (E) Immunoblot analysis of PKM2 in HL-1 nuclear and cytoplasmic extracts after treatment with DT for 4 h ($n = 3$). (F) PKM2 oligomerization in HL-1 cells after incubation with DT for 4 h ($n = 3$). (G) PKM2 activity in HL-1 cells after treatment with DT for 4 h ($n = 5$). (H) HL-1 cells were pre-treated with DT for 4 h, then, after washing, cells were incubated in glucose-free DMEM under 1% O_2 (OGD) for another 6 h and cell viability was measured by a CCK-8 assay ($n = 6$). The results are expressed as the mean ± SEM, except the proteome study (an unpaired two-tailed Student's t-test was used). $^*P < 0.05$, $^{**}P < 0.01$, $^{***}P < 0.001$. ns, statistically not significant.

immunofluorescence staining (Fig. 4B). In addition, an IP assay showed that DT increased the nuclear translocation of PKM2 and the binding between PKM2 and HIF-1α inside nucleus, but not in the DT plus Mito-T group (Fig. 4C). Induction of HIF-1α target genes by DT was also reversed by co-treatment with Mito-T (Fig. S4E). In support, low concentration H_2O_2 pretreatment increased HIF-1α accumulation dependent on PKM2 (Fig. 4D), and immunofluorescence confirmed the co-location in the nucleus (Fig. 4F). In addition, an IP assay showed that treatment with H_2O_2 facilitated the nuclear translocation of PKM2 and the binding between PKM2 and HIF-1α inside nucleus (Fig. 4G). A DSS cross-linking assay showed that H_2O_2 pre-treatment reduced PKM2 tetramer content with an increase in the formation of dimer (Fig. 4E), explaining the decrease in PK activity (Fig. 4H). H_2O_2

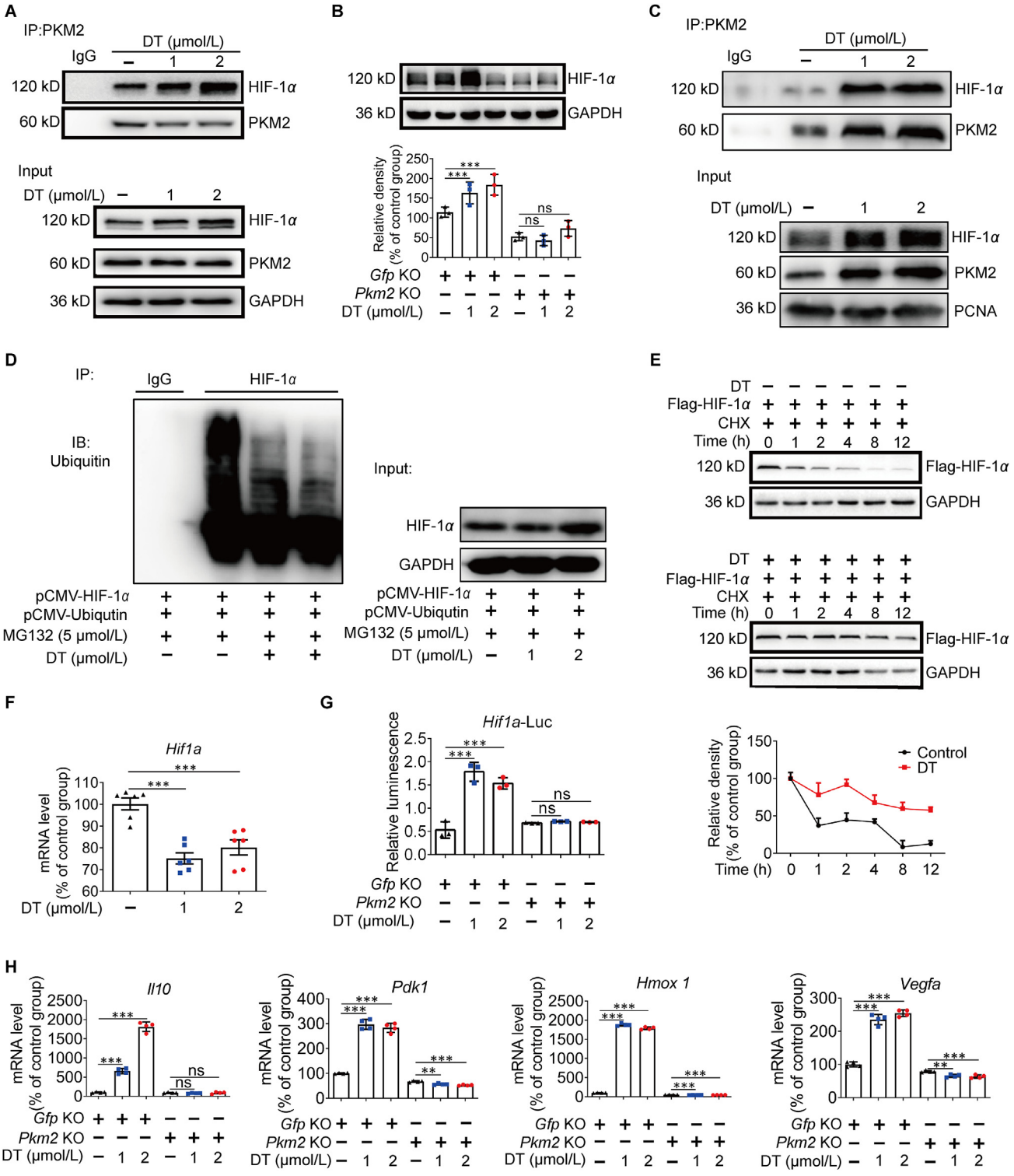

Figure 3 DT stabilizes HIF-1α. (A) IP analysis of the interaction between PKM2 and HIF-1α after incubation for 4 h ($n = 3$). (B) HIF-1α protein in *Pkm2* KO and *Gfp* KO cells treated with DT for 4 h ($n = 3$). (C) IP analysis of the interaction between PKM2 and HIF-1α in the nuclear after incubation for 4 h ($n = 3$). (D) IP analysis of the ubiquitination level of HIF-1α ($n = 3$). (E) Immunoblot analysis of Flag−HIF−1α in HEK293T cells (cycloheximide, CHX, 10 μg/mL) ($n = 3$). (F) mRNA level of *Hif1a* was determined by quantitative PCR after treatment with DT (1 and 2 μmol/L) or vehicle for 4 h ($n = 6$). (G) *Hif1a* luciferase activity in *Pkm2* or *Gfp* KO stable cell lines treated with DT for 4 h ($n = 3$). (H) mRNA level of *Il10*, *Pdk1*, *Hmox1* and *Vegfa* in HL-1 cells with DT for 4 h ($n = 4$). The results are expressed as the mean ± SEM. $^*P < 0.05$, $^{**}P < 0.01$, $^{***}P < 0.001$. ns, statistically not significant.

increased luciferase reporter activity of *Hif1a* with gene induction of *Il10*, *Hmox1*, *Pdk1* and *Vegfa*, which were diminished by *Pkm2* knockout (Fig. 4I and J). In support, the well-defined ROS inducers diamide and OGD insult promoted nuclear HIF-1α accumulation in a similar PKM2-dependent manner (Fig. S5C−S5F). Overall, these results suggest that the nuclear translocation of PKM2 and its interaction with HIF-1α are sensitive to ROS.

3.5. *Glutathionylation promotes PKM2 nuclear translocation*

Protein shuttle between the nucleus and cytoplasm is also regulated by post-translational modification[40]. PKM2 has been validated as a ROS sensor *via* the oxidation at Cys358, and is implicated in anti-oxidative responses[10]. ROS induces protein glutathionylation *via* direct oxidation of protein cysteines, which further react with GSSG to form the mixed disulfides. We wondered whether oxidized PKM2 may be sensitive to further glutathionylation. DT treatment increased the GSSG/GSH ratio in cultured cells (Fig. 5A), and exogenous GSSG supplement induced protein glutathionylation, indicated by α-GSH abundance (Fig. 5B). To verify that PKM2 was directly modified by GSSG, an IP assay of PKM2 was performed. As shown in Fig. 5C, treatment with GSSG increased PKM2 glutathionylation. Importantly, GSSG increased the content of PKM2 and HIF-1α in the nucleus (Fig. 5D). PKM2 and GSSG could present in the same complex that may contain other cellular proteins, such that the interaction is indirect. To further prove that GSSG could directly bind to PKM2, the cells were first treated with GSSG or vehicle, and a pull-down experiment was carried out. Results (Fig. 5E) show that biotin-labeled GSSG bound directly to PKM2, but the interaction was impaired by additional supplementation of unlabeled GSSG, indicating that unlabeled GSSG competed with

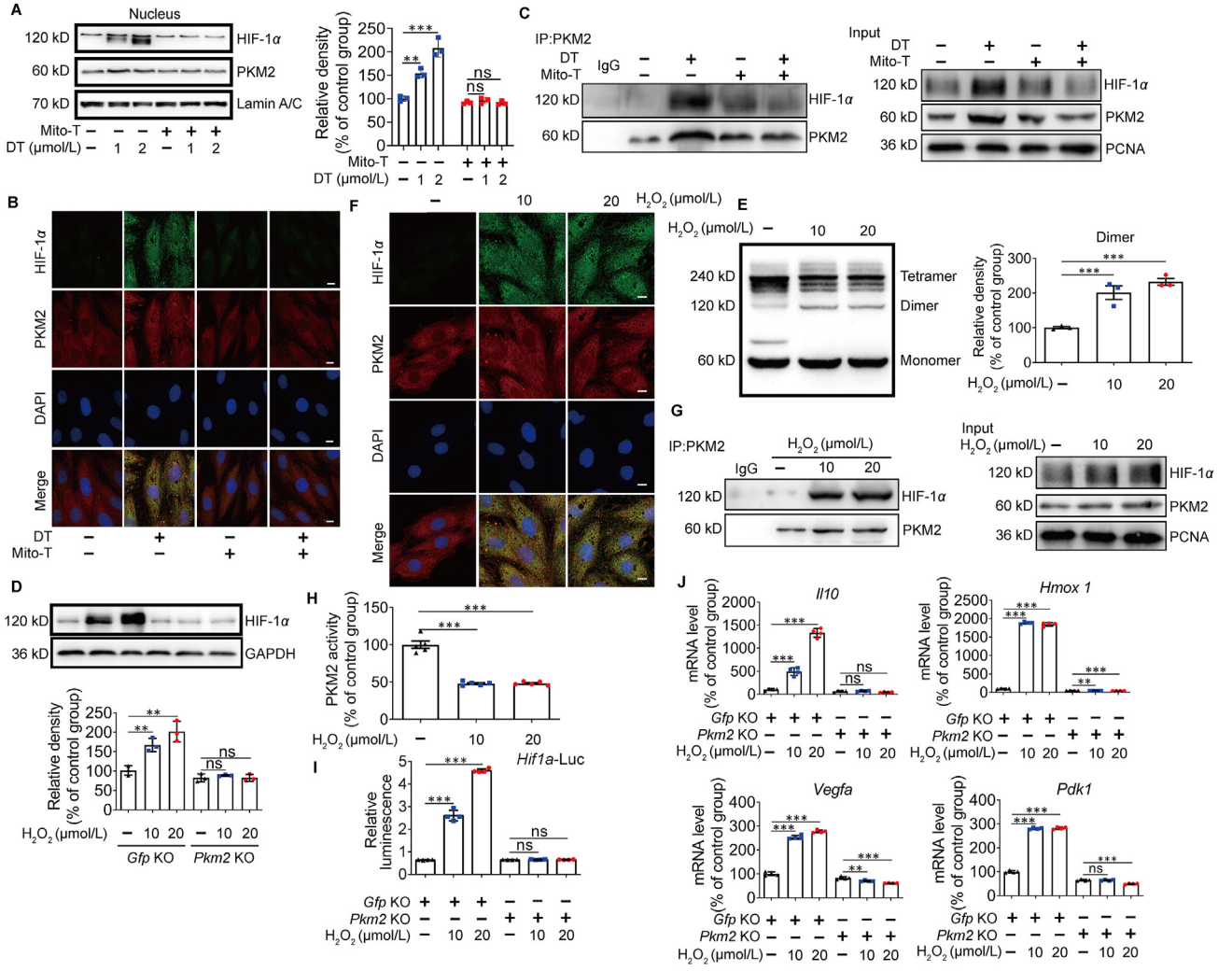

Figure 4 The preconditioning effect of DT depended on transient ROS generation. (A) Immunoblot analysis of nuclear PKM2 and HIF-1α in HL-1 cells treated with DT or Mito-Tempol (Mito-T) for 4 h ($n = 3$). (B) Endogenous HIF-1α and PKM2 in H9C2 cells treated with DT or Mito-T for 4 h (Scale bar: 10 μm, $n = 3$). (C) IP analysis of the interaction between PKM2 and HIF-1α in the nucleus ($n = 3$). (D) Immunoblot analysis of HIF-1α in HL-1 cells after treatment with H_2O_2 for 4 h ($n = 3$). (E) PKM2 oligomerization in HL-1 cells treated with H_2O_2 for 4 h ($n = 3$). (F) Endogenous HIF-1α and PKM2 in H9C2 cells treated with H_2O_2 for 4 h (Scale bar: 10 μm, $n = 3$). (G) IP analysis of the interaction between PKM2 and HIF-1α in the nucleus after incubation for 4 h ($n = 3$). (H) PKM2 activity in HL-1 cells treated with H_2O_2 for 4 h ($n = 5$). (I) *Hif1a* luciferase reporter in *Pkm2* or *Gfp* KO stable cells treated with H_2O_2 for 4 h ($n = 4$). (J) mRNA level of *Il10*, *Pdk1*, *Hmox1* and *Vegfa* in HL-1 cells treated with H_2O_2 for 4 h ($n = 4$). The results are expressed as the mean ± SEM. $^*P < 0.05$, $^{**}P < 0.01$, $^{***}P < 0.001$. ns, statistically not significant.

biotin-labeled GSSG to bind PKM2. In addition, a pull-down assay performed in a recombinant PKM2 system also supported the binding of GSSG to PKM2 (Fig. 5F). Overexpression of glutaredoxin 1 (Glrx1), an enzyme that catalyzes deglutathionylation, retarded PKM2 nuclear translocation and decreased nuclear HIF-1α (Fig. 5G). An IP assay of PKM2 confirmed that DT increased the content of glutathionylated PKM2 in the nucleus (Fig. 5H). These results indicate that by stimulating ROS production, DT consumed GSH to increase the formation of GSSG, which facilitated nuclear PKM2 translocation *via* glutathionylation modification.

3.6. *Cys423 and Cys424 of PKM2 are sensitive to glutathionylation*

Glutathione is predominately conjugated to cysteine of target proteins[41]. To identify the potential glutathionylation site, mutants of the ten known cysteines was carried out[42]. The flag-tagged wild-type or cysteine mutants were over-expressed in 293T cells. As shown in Supporting Information Fig. S6, mutation at C31, C49, C165, C317, C326, C358, C474 had negligible influence on DT-induced PKM2 accumulation in the nucleus, while the flag-tagged C152, C423 and C424 completely abolished this effect. It has been reported that C152 mutation facilitates PKM2 degradation[42] and thus, we focused on the amino acids at C423/424. A flag-tagged C423/424A double mutant form of PKM2 was constructed and over-expressed in 293T cells treatment with diamide or H_2O_2. Detection of nuclear fractions revealed that the flag-PKM2 nuclear translocation was increased in wild-type cells, but not in the mutant transfected-cells (Fig. 6A and B). In addition, we tested whether Cys423 and Cys424 of PKM2 could be modified by ROS. The DCP-Bio1 probe was used to detect cysteine oxidation (Fig. 6C). Like diamide and H_2O_2, DT treatment increased DCP-Bio1 binding to PKM2, but the interaction was impaired in *Pkm2* mutants (C423A, C424A and C423/424A) (Fig. 6D and E). An IP assay also confirmed that mutation of PKM2 at Cys423 and Cys424 sites reduced the glutathionylated form (Fig. 6F). A study by VanHecke[43] described a proteomics

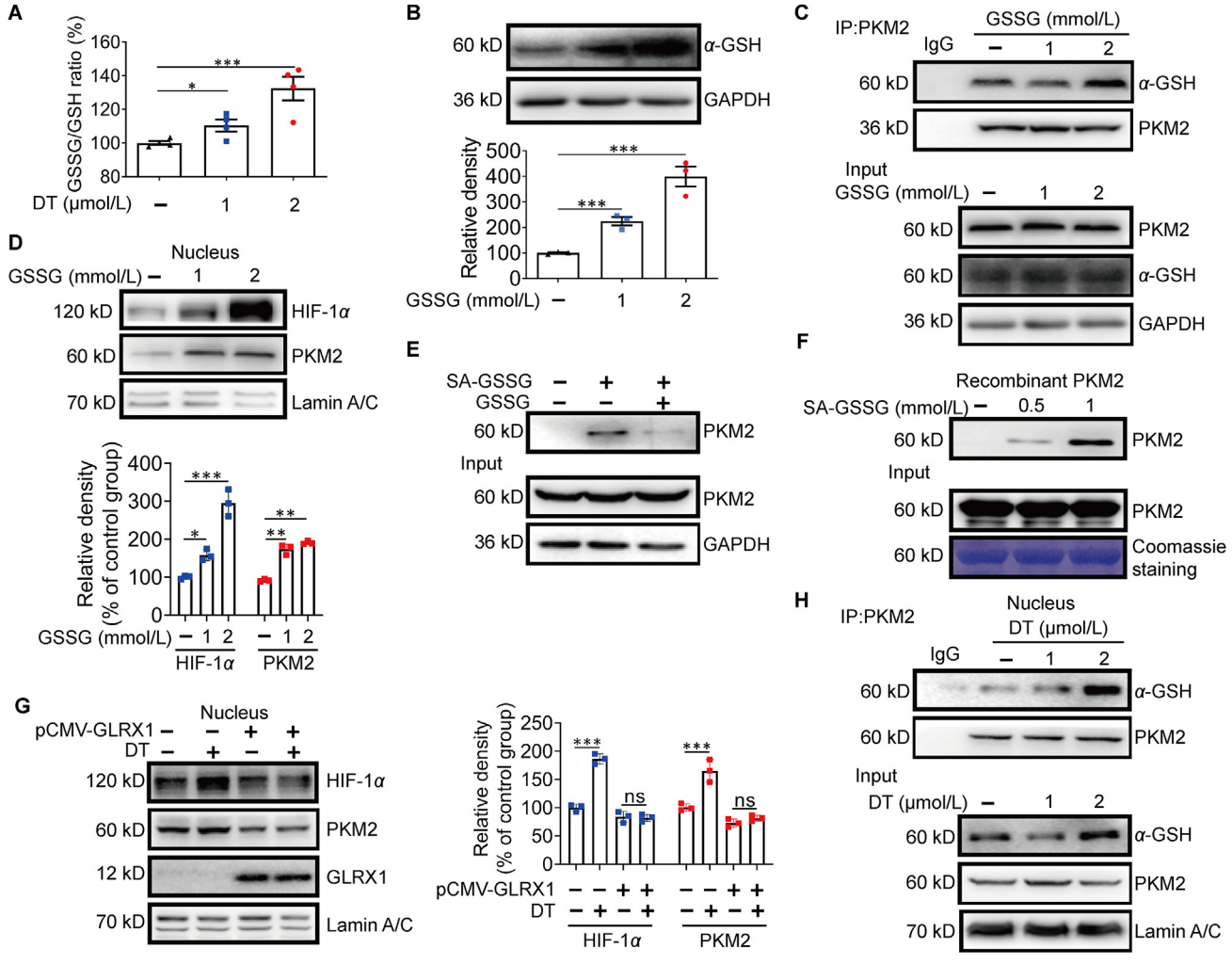

Figure 5 (A) The GSSG/GSH ratio in HL-cells treated with DT for 4 h ($n = 4$). (B) Immunoblot analysis of α-GSH after treatment with GSSG (1 and 2 mmol/L) for 4 h ($n = 3$). (C) IP analysis of the binding of α-GSH to PKM2 ($n = 3$). (D) Immunoblot analysis of HIF-1α and PKM2 in the nuclear fractions ($n = 3$). (E) HL-1 cells were pre-treated with GSSG, then an SA-GSSG pull down assay was performed and the pellet was detected by immunoblot ($n = 3$). (F) The pull-down assay was performed in a recombinant PKM2 system ($n = 3$). (G) Immunoblot analysis of HIF-1α, PKM2 and GLRX1 in the nuclear fractions ($n = 3$). (H) IP analysis of nuclear α-GSH and PKM2 in HL-1 cells treated with DT for 4 h ($n = 3$). The results are expressed as the mean ± SEM. $^*P < 0.05$, $^{**}P < 0.01$, $^{***}P < 0.001$.

study of protein glutathionylation in cardiomyocytes. We analyzed the raw data and identified two glutathionylation sites in PKM2 at Cys423 and Cys424. According to the semi-quantitative result, compared with the Cys423 site, the Cys424 site was more easily modified by glutathione (Fig. 6G). In addition, a docking study was performed and we found that GSSG docked closer to Cys424 than Cys423 (Fig. 6H). Together, our results indicate that glutathionylation of PKM2 at Cys423 and Cys424 facilitated tetramer-to-dimer conversion and the nuclear translocation of PKM2 for HIF-1α stabilization.

3.7. PKM2 glutathionylation is required for DT to prevent heart ischemic injury

We next sought to determine whether glutathionylation of PKM2 was an underlying mechanism for the IPC effects of DT *in vivo*. To this end, we delivered adeno-associated virus (AAV)-expressing shRNA, wild-type and C423/424A mutant forms of *Pkm2* to mice, and cardiac knockdown or overexpression efficiency was verified (Supporting Information Fig. S7A and S7C). We first examined preconditioning regulation in the heart before surgery after treatment with DT for 3 days (10 mg/kg). DT pretreatment increased PKM2 glutathionylation and nuclear HIF-1α accumulation with gene induction of *Il10*, *Hmox1*, *Pdk1* and *Vegfa,* which were attenuated by *Pkm2* knockdown or C423/424 mutation (Fig. 7A–C). As expected, DT preconditioning reduced myocardial infarction in a similar way in mice after permanent coronary ligation (Fig. 7D, Fig. S7B). Hemodynamics observed three weeks post-infarction was reported to be negatively correlated with initial ischemic injury[44]. To verify whether DT preconditioning had a contribution to improving the prognosis after cardiac ischemia, left ventricular function was examined in mice three weeks after surgery (Fig. S7B). H&E staining and Masson staining showed that DT normalized myocardial structure and prevented collagen deposition, but these protective effects were attenuated by *Pkm2* knockdown. To further demonstrate that cysteine 423/424 was critical for these beneficial effects, we restored the level of *Pkm2* in heart by over-expressing either the wild-type *Pkm2* or the C423/424A mutant *via* AAV-mediated transfection. Although the expression level of *Pkm2* was rescued, the protective effects of DT were diminished by C423/424A mutation (Fig. 7E and Fig. S7D). When heart contractile function was impaired by ischemic insult, DT restored the loss of ejection fractions (EF) and shortening fraction (FS) in wild-type or *Pkm2* over-expressing mice, but not in *Pkm2* knock down or mutation mice (Fig. 7F and G). Detection of CK-MB, LDH, and cTn-I in serum further supported the preconditioning role of DT in cardioprotection (Fig. S7E). These data collectively demonstrate that DT preconditioned the heart against ischemic injury and could improve the recovery after ischemic injury.

4. Discussion

Preconditioning protection has been viewed as an important intervention to attenuate ischemia and reperfusion damage. Our previous study showed that DT preconditioned the heart against reperfusion injury *via* upregulation of HIF-1α-mediated antioxidative defense[28]. However, the exact mechanisms underlying how DT and DT-triggered transient ROS signals precondition the myocardium *via* stabilizing HIF-1α remains unclear. This study highlights the regulatory role of ROS-mediated PKM2 nuclear translocation and illustrates the molecular mechanism through which PKM2 is glutathionylated and thereby stabilizes HIF-1α. Our study shows how PKM2 senses ROS signals *via* a mechanism of posttranslational modification, thereby adding new evidence in support of ROS as key IPC signals.

Similar to a low concentration of H_2O_2, DT pretreatment protected cells from OGD insult, and this action was dependent on transient ROS production, because co-treatment with antioxidant agents diminished its protective effects. The preconditioning effect was also confirmed in rats subjected to ISO challenge. ISO challenge induces heart injury, and increased oxygen consumption and thrombosis formation are the main causes[30]. In this sense, ISO challenge provides a feasible and non-invasive model which produces myocardial damage similar to that seen in acute cardiac ischemia in humans[45]. These results *in vitro* and *in vivo* provide evidence to support the preconditioning role of DT in cardioprotection.

Through proteomics analysis, PKM2 has emerged as an important mediator responsible for DT-mediated preconditioning regulation. PKM2 possesses metabolic and nonmetabolic properties dependent on its subcellular location[46]. The shuttling of PKM2 between the cytosol and nucleus is regulated by tetramer and dimer dynamics. After preparation of the nuclear and cytoplasmic fractions using size-exclusion chromatography, gel filtration chromatography revealed that nuclear PKM2 is only in the dimer form, while the cytoplasmic PKM2 exists in both dimer and tetramer form[46]. PKM2 in the cytoplasm efficiently promotes glycolysis and energy production, whereas PKM2 in the dimer state can enter the nucleus to regulate gene expression. The dissociation of PKM2 into dimer is reversible in normally dividing cells, as the dimers assemble to high-affinity tetramers and recover with full enzymatic activity to produce energy (ATP)[47]. In fact, the dynamic equilibrium between tetramer and dimer maintains a balance between anabolic and catabolic phases of cell metabolism. A previous study reported that oxidative modification of PKM2 Cys358 degrades PKM2 from the tetrameric form to the dimer form and inhibit its catalytic activity, which allows the diversion of glucose-6-phosphate into the pentose phosphate pathway[10]. Herein, we show that transient ROS triggers PKM2 glutathionylation which stabilizes HIF-1α, thereby preconditioning the myocardium against ischemic injury in a non-metabolic regulatory mode. We found that DT increased HIF-1α nuclear accumulation and transcriptional activity in the context of nuclear PKM2, consistent with a published study that demonstrates that in the nucleus, PKM2 functions together with HIF-1α[17,34].

HIF-1α is an oxygen-sensitive transcriptional activator that is activated under hypoxic conditions for transcriptional regulation of genes encoding proteins involved in metabolism and cell survival[15,16]. HIF-1α enhances glycolytic flux, promotes angiogenesis and increases mitochondrial antioxidant production, mediating adaptive responses to hypoxia from different approaches[23]. Gene induction of *Hmox1*, *Pdk1*, *Il10* and *Vegfa* during prolonged hypoxia is involved in the adaptive response, contributing to IPC protection *via* different mechanisms. Ischemia boosts ROS production, while HO-1 (encoded by *Hmox1*) is an antioxidant protein in the intrinsic defense system, and protects cell from injury by combating oxidative stress[48]. PDK1 (encoded by *Pdk1*) is essential to preserve physiological cardiac resistance to metabolic stress by reducing mitochondrial ROS production[49]. IL10 (encoded by *Il10*) induction in the infarcted heart attenuates inflammatory response[50]. VEGFA (encoded by *Vegfa*) stimulates cardiac stem cell migration, mobilization and myocardial repair within infarcted heart tissue[51]. PKM2 binds and stabilizes HIF-1α protein in the nucleus, and it is rational to believe that induction of

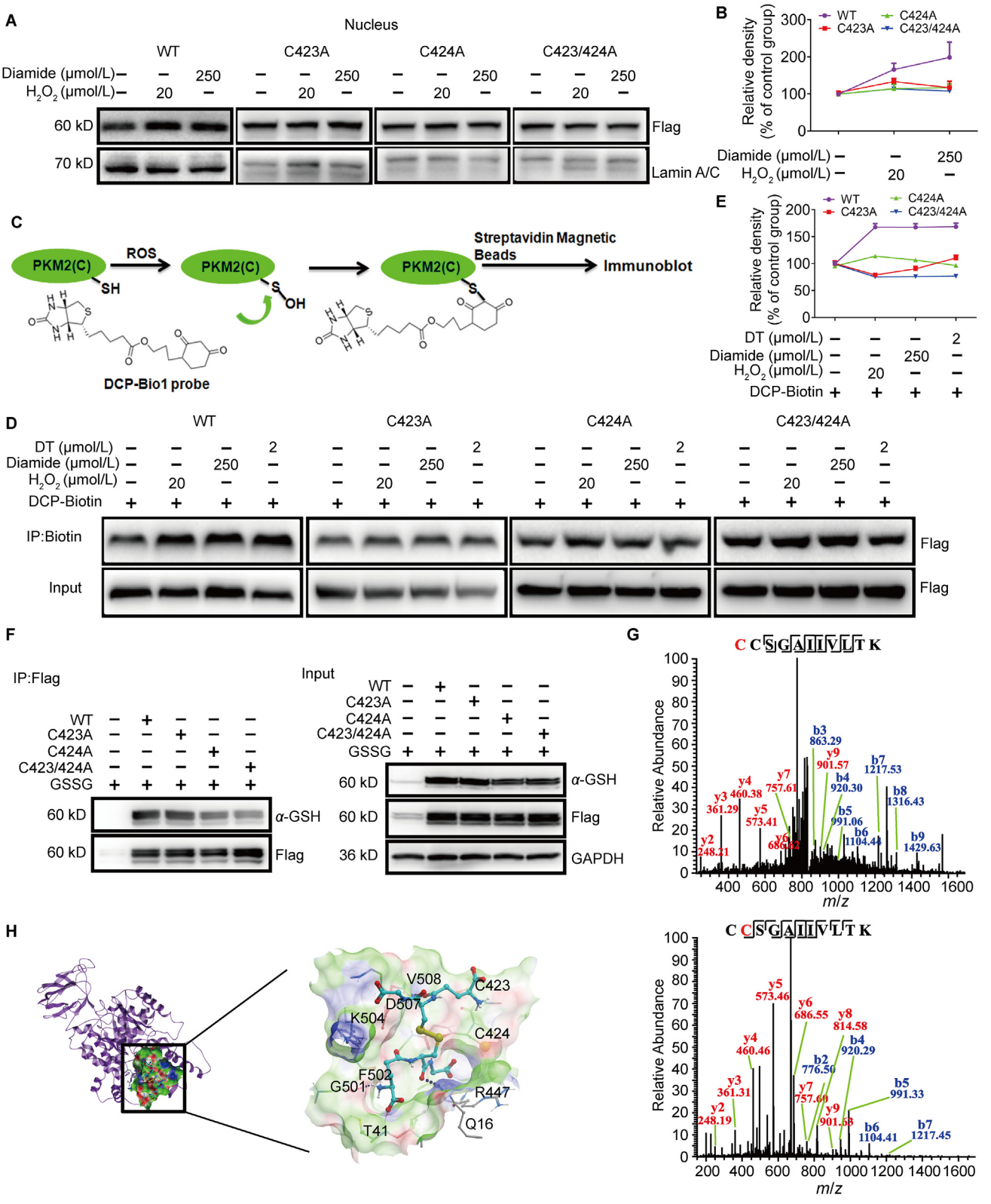

Figure 6 Characterization of the PKM2 glutathionylation amino acid sites. Immunoblot analysis of nuclear PKM2 in HEK-293T cells (A) and quantitative results (B) in HEK-293T cells pre-treated with diamide or H_2O_2 for 4 h ($n = 3$). (C) A scheme showing how the DCP-Bio1 probe detects the oxidation of Cys423/424 in PKM2. (D) Immunoblot analysis of PKM2 protein level pulled out by DCP-Bio1 probe in HEK 293T cells treated with H_2O_2, diamide or DT for 4 h ($n = 3$). (E) Quantitative analysis of the PKM2 protein level pulled out by DCP-Bio1 probe ($n = 3$). (F) IP analysis of Flag-PKM2 and mutants. (G) LC−MS/MS analysis of PKM2 glutathionylation in HL-1 cells. The amino acid site Cys423 and Cys424 were modified by GSSG (data from Project PXD012171). (H) A structural model of GSSG binding to PKM2. GSSG is docked to the disulfide bond of Cys423 and Cys424. The hydrogen bonds formed at G501, K504 and R447 between GSSG and PKM2.

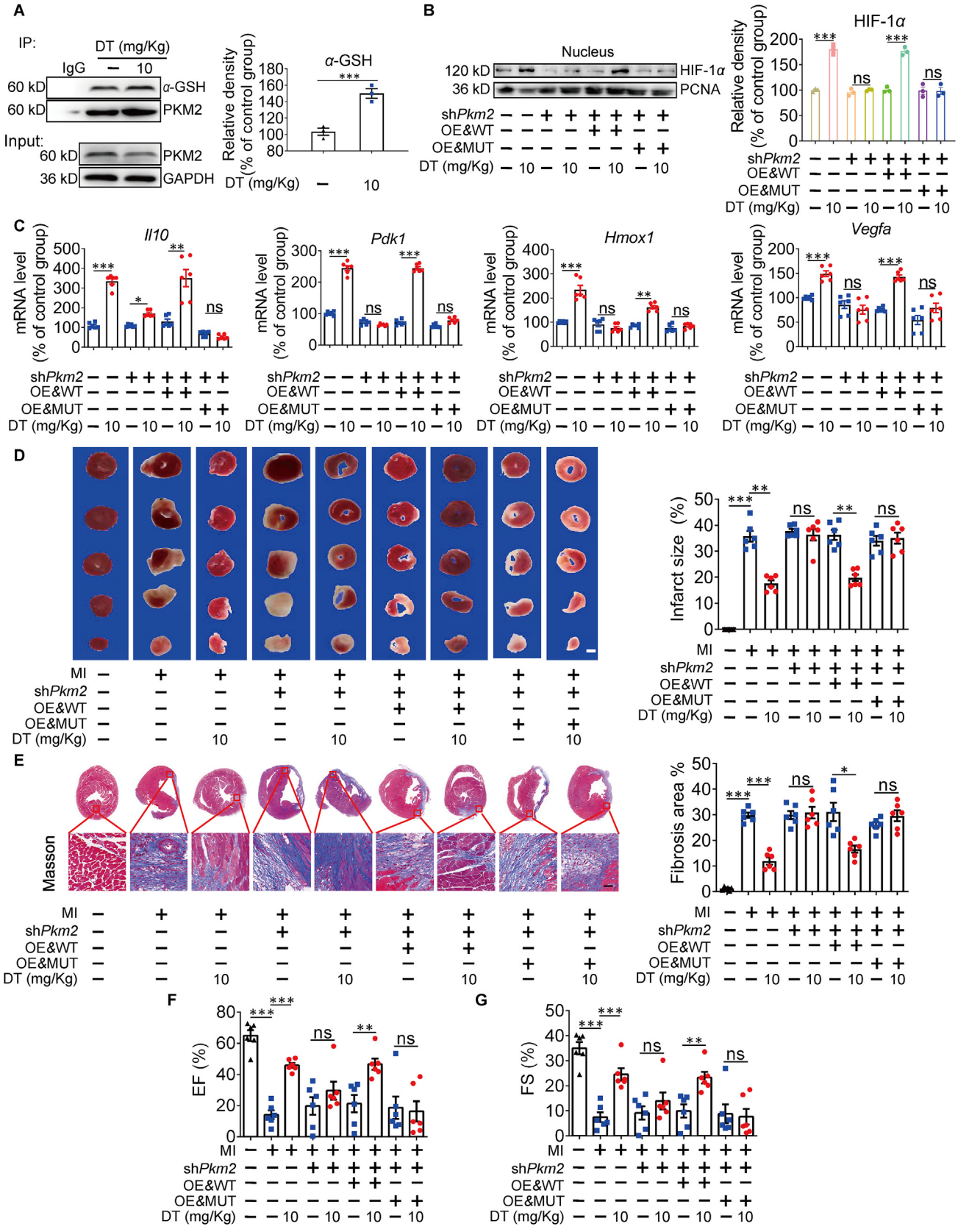

Figure 7 The preconditioning effect of DT in mice. (A) IP analysis of the binding of α-GSH to PKM2 and quantitative results ($n = 3$). (B) Immunoblot analysis of HIF-1α and quantitative results in the nuclear fractions of mouse heart ($n = 3$). (C) mRNA level of *Pdk1*, *Hmox1*, *Vegfa* and *Il10* in the heart ($n = 6$). Myocardial infarction in mice after coronary ligation without reperfusion was examined three days after ligation. (D) Representative images and calculated infarct size of the myocardium (Scale bar: 2 mm, $n = 6$). The effects on myocardial injury, fibrosis and ventricular function were examined 3 weeks after the surgery. (E) Masson staining of heart sections and quantitative fibrotic area (Scale bar: 50 μm, $n = 6$). (F) Ejection fraction (EF) ($n = 6$). (G) Fractional shortening (FS) ($n = 6$). The results are expressed as the means and SEM. $^*P < 0.05$, $^{**}P < 0.01$, $^{***}P < 0.001$. ns, statistically not significant.

its target gene, such as *Hmox1*, *Pdk1*, *Il10* and *Vegfa*, has a contribution to the preconditioning protection, largely due to adaptive responses to maintain cell survival.

Although we show that induction of PKM2/HIF-1α signaling cascades in DT-mediated preconditioning protection, we cannot exclude the involvement of PI3K/Akt and MAPK pathways. PI3K and Akt serve as survival kinases in IPC[52]. Akt is a downstream kinase of PI3K activation and IPC induces Akt phosphorylation to confer protection *via* upregulation of PKC-ε and NO production[53]. The role of MAPK as a potential mediator of protection in IPC has been well documented, although several studies failed to demonstrate a role[53]. In fact, the IPC effects of PI3K−Akt and MAPK signaling also require HIF-1α, and there are several overlaps among these pathways[54].

As myocardial infarction and necrosis are irreversible and preconditioning treatment is proposed to improve the prognosis of myocardial infarction[55], we observed the effect of IPC in mice three weeks after coronary artery ligation. As expected, pretreatment with DT attenuated heart ischemic injury and improved cardiac contractive function in a manner dependent on PKM2. Mutation of PKM2 at Cys423/Cys424 diminished the beneficial effects, indicating that PKM2 glutathionylation is necessary for the preconditioning protection. Moreover, these results also indicate the potential role of HIF-1α signaling cascades in heart protection. Although preconditioning protection against ischemic injury can improve heart contractive function during the prognosis after ischemia, we should note that more pathological factors are integrated in heart failure and mitochondrial dysfunction and metabolic disorders are the important causes of impaired heart function[56]. IPC attenuates ischemic injury by improving adaptive responses from different aspects, and the integrated role in the protection of ventricular contractive function is a subject remaining to be investigated.

5. Conclusions

Our study demonstrates that PKM2 is sensitive to alteration of cellular redox status. By increasing modest ROS production, DT induces PKM2 glutathionylation to facilitate nuclear translocation in dimer form. In the nucleus, PKM2 interacts with HIF-1α and downstream transcriptional regulation contributes to IPC protection. This finding expands our knowledge on oxidative modification of PKM2, and indicates the potential of IPC in the protection of heart ischemic injury without reperfusion.

Acknowledgments

This work was supported by the National Key R&D Program of China (2019YFC1711000), the National Natural Science Foundation of China (No.81421005) and the “111” Project (B16046) from the Ministry of Education of China and the State Administration of Foreign Experts Affairs of China.

Author contributions

Ping Li, Haiping Hao and Hua Yang designed the research. Xunxun Wu, Lian Liu, Qiuling Zheng and Hui Ye performed the research. Xunxun Wu and Haiping Hao wrote the paper. Hui Ye, Hua Yang, Haiping Hao and Ping Li reviewed and modified the paper.

Conflicts of interest

The authors declare no conflicts of interest.

Appendix A. Supporting information

Supporting data to this article can be found online at https://doi.org/10.1016/j.apsb.2022.07.006.

References

1. Hausenloy DJ, Yellon DM. Myocardial ischemia−reperfusion injury: a neglected therapeutic target. *J Clin Invest* 2013;**123**:92−100.
2. Murry CE, Jennings RB, Reimer KA. Preconditioning with ischemia: a delay of lethal cell injury in ischemic myocardium. *Circulation* 1986;**74**:1124−36.
3. Hausenloy DJ, Barrabes JA, Bøtker HE, Davidson SM, Di Lisa F, Downey J, et al. Ischaemic conditioning and targeting reperfusion injury: a 30 year voyage of discovery. *Basic Res Cardiol* 2016;**111**:70.
4. Heusch G. Cardioprotection: chances and challenges of its translation to the clinic. *Lancet* 2013;**381**:166−75.
5. Shereif H, Rezkalla RAK. No-reflow phenomenon. *Circulation* 2002;**105**:656−62.
6. Yip HK, Chen MC, Chang HW, Hang CL, Hsieh YK, Fang CY, et al. Angiographic morphologic features of infarct-related arteries and timely reperfusion in acute myocardial infarction: predictors of slow-flow and no-reflow phenomenon. *Chest* 2002;**122**:1322−32.
7. Hale SL, Herring MJ, Kloner RA. Delayed treatment with hypothermia protects against the no-reflow phenomenon despite failure to reduce infarct size. *J Am Heart Assoc* 2013;**2**:e004234.
8. Niccoli G, Burzotta F, Galiuto L, Crea F. Myocardial no-reflow in humans. *J Am Coll Cardiol* 2009;**54**:281−92.
9. Palsson-McDermott EM, Curtis AM, Goel G, Lauterbach MAR, Sheedy FJ, Gleeson LE, et al. Pyruvate kinase M2 regulates Hif-1α activity and IL-1β induction and is a critical determinant of the warburg effect in LPS-activated macrophages. *Cell Metab* 2015;**21**:65−80.
10. Anastasiou D, Poulogiannis G, Asara JM, Boxer MB, Jiang Jk, Shen M, et al. Inhibition of pyruvate kinase M2 by reactive oxygen species contributes to cellular antioxidant responses. *Science* 2011;**334**:1278−83.
11. Chen D, Wei L, Liu ZR, Yang JJ, Gu X, Wei ZZ, et al. Pyruvate kinase M2 increases angiogenesis, neurogenesis, and functional recovery mediated by upregulation of STAT3 and focal adhesion kinase activities after ischemic stroke in adult mice. *Neurotherapeutics* 2018;**15**:770−84.
12. Magadum A, Singh N, Kurian AA, Munir I, Mehmood T, Brown K, et al. Pkm2 regulates cardiomyocyte cell cycle and promotes cardiac regeneration. *Circulation* 2020;**141**:1249−65.
13. Alquraishi M, Puckett DL, Alani DS, Humidat AS, Frankel VD, Donohoe DR, et al. Pyruvate kinase M2: a simple molecule with complex functions. *Free Radic Biol Med* 2019;**143**:176−92.
14. Steták A, Veress R, Ovádi J, Csermely P, Kéri G, Ullrich A. Nuclear translocation of the tumor marker pyruvate kinase M2 induces programmed cell death. *Cancer Res* 2007;**67**:1602−8.
15. Kelly B, O'Neill LA. Metabolic reprogramming in macrophages and dendritic cells in innate immunity. *Cell Res* 2015;**25**:771−84.
16. Yee Koh M, Spivak-Kroizman TR, Powis G. HIF-1 regulation: not so easy come, easy go. *Trends Biochem Sci* 2008;**33**:526−34.
17. Luo W, Hu H, Chang R, Zhong J, Knabel M, O'Meally R, et al. Pyruvate kinase M2 is a PHD3-stimulated coactivator for hypoxia-inducible factor 1. *Cell* 2011;**145**:732−44.
18. Kalogeris T, Bao Y, Korthuis RJ. Mitochondrial reactive oxygen species: a double edged sword in ischemia/reperfusion *vs* preconditioning. *Redox Biol* 2014;**2**:702−14.

19. Tritto I, D'Andrea D, Eramo N, Scognamiglio A, De Simone C, Violante A, et al. Oxygen radicals can induce preconditioning in rabbit hearts. *Circ Res* 1997;**80**:743−8.
20. Baines CP, Goto M, Downey JM. Oxygen radicals released during ischemic preconditioning contribute to cardioprotection in the rabbit myocardium. *J Mol Cell Cardiol* 1997;**29**:207−16.
21. Berra E, Roux D, Richard DE, Pouysségur J. Hypoxia-inducible factor-1 alpha (HIF-1 alpha) escapes O_2-driven proteasomal degradation irrespective of its subcellular localization: nucleus or cytoplasm. *EMBO Rep* 2001;**2**:615−20.
22. Niecknig H, Tug S, Reyes BD, Kirsch M, Fandrey J, Berchner-Pfannschmidt U. Role of reactive oxygen species in the regulation of HIF-1 by prolyl hydroxylase 2 under mild hypoxia. *Free Radic Res* 2012;**46**:705−17.
23. Semenza GL. Hypoxia-inducible factors: coupling glucose metabolism and redox regulation with induction of the breast cancer stem cell phenotype. *EMBO J* 2017;**36**:252−9.
24. Zhang J, Ye ZW, Singh S, Townsend DM, Tew KD. An evolving understanding of the *S*-glutathionylation cycle in pathways of redox regulation. *Free Radic Biol Med* 2018;**120**:204−16.
25. Wang L, Ma R, Liu C, Liu H, Zhu R, Guo S, et al. *Salvia miltiorrhiza*: a potential red light to the development of cardiovascular diseases. *Curr Pharm Des* 2017;**23**:1077−97.
26. Han JY, Fan JY, Horie Y, Miura S, Cui DH, Ishii H, et al. Ameliorating effects of compounds derived from *Salvia miltiorrhiza* root extract on microcirculatory disturbance and target organ injury by ischemia and reperfusion. *Pharmacol Ther* 2008;**117**:280−95.
27. Li Z, Zou J, Cao D, Ma X. Pharmacological basis of tanshinone and new insights into tanshinone as a multitarget natural product for multifaceted diseases. *Biomed Pharmacother* 2020;**130**:110599.
28. Jiang L, Zeng H, Ni L, Qi L, Xu Y, Xia L, et al. HIF-1alpha preconditioning potentiates antioxidant activity in ischemic injury: the role of sequential administration of dihydrotanshinone I and protocatechuic aldehyde in cardioprotection. *Antioxid Redox Signal* 2019;**31**:227−42.
29. Zeng H, Wang L, Zhang J, Pan T, Yu Y, Lu J, et al. Activated PKB/GSK-3beta synergizes with PKC-delta signaling in attenuating myocardial ischemia/reperfusion injury *via* potentiation of NRF2 activity: therapeutic efficacy of dihydrotanshinone-I. *Acta Pharm Sin B* 2021;**11**:71−88.
30. Garg M, Khanna D. Exploration of pharmacological interventions to prevent isoproterenol-induced myocardial infarction in experimental models. *Ther Adv Cardiovasc Dis* 2014;**8**:155−69.
31. Zeng B, Tong S, Ren X, Xia H. Cardiac cell proliferation assessed by EdU, a novel analysis of cardiac regeneration. *Cytotechnology* 2016;**68**:763−70.
32. Lai TC, Lee TL, Chang YC, Chen YC, Lin SR, Lin SW, et al. MicroRNA-221/222 mediates ADSC-exosome-induced cardioprotection against ischemia/reperfusion by targeting PUMA and ETS-1. *Front Cell Dev Biol* 2020;**8**:569150.
33. Hausenloy DJ, Yellon DM. The second window of preconditioning (SWOP) where are we now?. *Cardiovasc Drugs Ther* 2010;**24**:235−54.
34. Christofk HR, Vander Heiden MG, Harris MH, Ramanathan A, Gerszten RE, Wei R, et al. The M2 splice isoform of pyruvate kinase is important for cancer metabolism and tumour growth. *Nature* 2008;**452**:230−3.
35. Zhu Y, Zhang Y, Ojwang BA, Brantley MA, Gidday JM. Long-term tolerance to retinal ischemia by repetitive hypoxic preconditioning: role of HIF-1alpha and heme oxygenase-1. *Invest Ophthalmol Vis Sci* 2007;**48**:1735−43.
36. Cai ZP, Parajuli N, Zheng X, Becker L. Remote ischemic preconditioning confers late protection against myocardial ischemia−reperfusion injury in mice by upregulating interleukin-10. *Basic Res Cardiol* 2012;**107**:277.
37. Yang W, Zheng Y, Xia Y, Ji H, Chen X, Guo F, et al. ERK1/2-dependent phosphorylation and nuclear translocation of PKM2 promotes the Warburg effect. *Nat Cell Biol* 2012;**14**:1295−304.
38. Chachami G, Paraskeva E, Mingot JM, Braliou GG, Gorlich D, Simos G. Transport of hypoxia-inducible factor HIF-1alpha into the nucleus involves importins 4 and 7. *Biochem Biophys Res Commun* 2009;**390**:235−40.
39. Semenza GL. Hypoxia-inducible factors: mediators of cancer progression and targets for cancer therapy. *Trends Pharmacol Sci* 2012;**33**:207−14.
40. Ptak C, Wozniak RW. SUMO and nucleocytoplasmic transport. *Adv Exp Med Biol* 2017;**963**:111−26.
41. Mailloux RJ. Protein *S*-glutathionylation reactions as a global inhibitor of cell metabolism for the desensitization of hydrogen peroxide signals. *Redox Biol* 2020;**32**:101472.
42. Zhou HL, Zhang R, Anand P, Stomberski CT, Qian Z, Hausladen A, et al. Metabolic reprogramming by the *S*-nitroso-CoA reductase system protects against kidney injury. *Nature* 2019;**565**:96−100.
43. VanHecke GC, Abeywardana MY, Ahn YH. Proteomic identification of protein glutathionylation in cardiomyocytes. *J Proteome Res* 2019;**18**:1806−18.
44. Pfeffer JM, Pfeffer MA, Braunwald E. Influence of chronic captopril therapy on the infarcted left ventricle of the rat. *Circ Res* 1985;**57**:84−95.
45. Wong ZW, Thanikachalam PV, Ramamurthy S. Molecular understanding of the protective role of natural products on isoproterenol-induced myocardial infarction: a review. *Biomed Pharmacother* 2017;**94**:1145−66.
46. Gao X, Wang H, Yang JJ, Liu X, Liu ZR. Pyruvate kinase M2 regulates gene transcription by acting as a protein kinase. *Mol Cell* 2012;**45**:598−609.
47. Wu X, Liu L, Zheng Q, Hao H, Ye H, Li P, et al. Protocatechuic aldehyde protects cardiomyocytes against ischemic injury *via* regulation of nuclear pyruvate kinase M2. *Acta Pharm Sin B* 2021;**11**:3553−66.
48. Wu ML, Ho YC, Yet SF. A central role of heme oxygenase-1 in cardiovascular protection. *Antioxid Redox Signal* 2011;**15**:1835−46.
49. Budas GR, Sukhodub A, Alessi DR, Jovanović A. 3′Phosphoinositide-dependent kinase-1 is essential for ischemic preconditioning of the myocardium. *FASEB J* 2006;**20**:2556−8.
50. Frangogiannis NG. Pathophysiology of myocardial infarction. *Compr Physiol* 2015;**5**:1841−75.
51. Braile M, Marcella S, Cristinziano L, Galdiero MR, Modestino L, Ferrara AL, et al. VEGF-A in cardiomyocytes and heart diseases. *Int J Mol Sci* 2020;**21**:5294.
52. Hausenloy DJ, Yellon DM. Survival kinases in ischemic preconditioning and postconditioning. *Cardiovasc Res* 2006;**70**:240−53.
53. Tong H, Chen W, Steenbergen C, Murphy E. Ischemic preconditioning activates phosphatidylinositol-3-kinase upstream of protein kinase C. *Circ Res* 2000;**87**:309−15.
54. Lecour S. Multiple protective pathways against reperfusion injury: a SAFE path without Aktion?. *J Mol Cell Cardiol* 2009;**46**:607−9.
55. Colonna P, Cadeddu C, Montisci R, Ruscazio M, Selem AH, Chen L, et al. Reduced microvascular and myocardial damage in patients with acute myocardial infarction and preinfarction angina. *Am Heart J* 2002;**144**:796−803.
56. Murphy MP, Hartley RC. Mitochondria as a therapeutic target for common pathologies. *Nat Rev Drug Discov* 2018;**17**:865−86.